Characterization and Fungicide Sensitivity of Two *Fusarium spp.* Associated With Stem Rot of Dragon Fruit in Guizhou, China

Jin Zhao * and Miao Huang

Posted Date: 1 November 2023

doi: 10.20944/preprints202310.1930.v1

Keywords: dragon fruit; stem rot; Fusarium; identification; fungicides

Article

Characterization and Fungicide Sensitivity of Two *Fusarium* spp. Associated with Stem Rot of Dragon Fruit in Guizhou, China

Jin Zhao [1,2,*] and Miao Huang [1,2]

[1] College of Agriculture, Guizhou University; Guiyang 550025
[2] Institute of Pepper Industry and Technology, Guizhou University; Guiyang 550025
* Correspondence: zhaojin7094@163.com; Tel.: +86 18985183317

Abstract: Dragon fruit (*Hylocereus polyrhizus*) constitutes an important economic industry in Guizhou Province, China; however, in recent years, stem rot in this region has become increasingly severe. Moreover, the pathogens responsible for stem rot in Guizhou and their sensitivity to fungicides remain elusive. Therefore, in this study, we aimed to determine the causative pathogens of stem rot in this region and analyze their sensitivity to fungicides. Twenty-four isolates were obtained from diseased tissues, from which H-4 and H-5 were selected and confirmed as pathogens. Based on the morphological characteristics of macroconidia, microconidia, and colony morphology, the polygenic phylogenetic tree constructed using internal transcribed spacer, elongation factor 1-alpha, and retinol-binding protein-2 gene fragments, along with carbon source metabolism using FF microplates, the two pathogens were identified as *Fusarium oxysporum* and *F. concentricum* respectively. In addition, the in vitro toxicity of eight fungicides against both pathogens were measured based on mycelium growth rate. The results showed that 75% trifloxystrobin·tebuconazole exhibited the strongest inhibitory effect on both isolates, with concentration for 50% of maximum effect values of 0.1262 μg/mL and 0.1385 μg/mL, respectively. This study identified two *Fusarium* spp. as the causative pathogens of stem rot in dragon fruit, with *F. concentricum* being reported for the first time, and demonstrated the best fungicide for them. These findings hold significant potential for guiding the effective treatment of stem rot in dragon fruit in Guizhou, China.

Keywords: dragon fruit; stem rot; *Fusarium*; identification; fungicides

1. Introduction

Dragon fruit or pitaya (*Hylocereus polyrhizus*) is a tropical and subtropical herbaceous fruit tree that belongs to the family Cactaceae and the genus *Hylocereus* [1]. The fruit enjoys popularity among consumers worldwide and holds substantial economic value because it is rich in iron, phosphorus, and other trace elements, as well as pulp fiber and carotene [2,3]. Originating in Central America, the cultivation of dragon fruit has gradually expanded since the 1990s to numerous provinces in southern China, including Guizhou Province, where small-scale cultivation began in 2001 [4]. The dragon tree swiftly gained prominence as an essential asset for local development owing to its suitability for open-air planting, resistance to barren conditions and drought, and high economic value. In 2020, the cultivated area in Guizhou Province exceeded 6,700 ha, and its output reached 80,000 tons, ranking among the highest in China [5]. However, the expansion of cultivation areas, coupled with rising temperatures and increased rainfall, has led to a notable surge in the occurrence of fungal diseases affecting dragon fruit in Guizhou, ultimately affecting their economic benefits [6,7].

Dragon fruit is susceptible to over seven fungus-related diseases, including canker and anthracnose, with stem rot being prevalent [8–10]. Stem rot has become widespread across all planting regions in Guizhou Province, resulting in significant yield reduction and, in severe cases, crop failure [11]. This disease is easily disseminated through wind or rain, specifically during hot and rainy weather conditions [12]. The symptoms of this disease progress in distinct stages, starting with small brown patches on the stem that gradually spread throughout the plant. As the disease

 doi:10.20944/preprints202310.1930.v1

advances, the late-stage lesion transitions from green to a dark yellow color, developing penetrating and translucent characteristics with soft tissue rot [13]. Currently, there are conflicting reports regarding the pathogens responsible for stem rot in China. Several fungi, including *Enterbacter* sp., *Bipolaris cactivora*, *Neoscytalidium dimidiatum*, *Fusarium semitectum*, F. *oxysporum*, and F. *moniliforme* are speculated to be the major contributors [8,14–16]. Establishing pathogen clarity is essential for effective disease management for both farmers and plant caretakers. Therefore, a comprehensive understanding of the specific pathogenic species associated with local stem rot is critical.

Despite the adverse environmental effects associated with the use of fungicides, including trifloxystrobin (FRAC 11), tebuconazole (FRAC 3), and difenoconazole (FRAC 3), they remain the most effective method for controlling stem rot in dragon fruit [17,18]. However, many studies have reported an increase in the fungicide-resistant strains of several types of pathogens [19]. Notably, the major plant pathogen F. oxysporum, which affects tomatoes, potatoes, dragon fruit, and other commercial crops, has demonstrated resistance to various agents, including difenoconazole and tebuconazole [20,21]. Understanding the sensitivity of pathogens to various fungicides and employing appropriate doses are critical for effective chemical control of the disease, as well as environmental protection. However, the pathogens responsible for stem rot in Guizhou, China and their sensitivity to fungicides remain unclear.

In this study, we obtained stem rot samples from dragon fruit in Guizhou Province, isolated fungi from affected tissues, and used Koch's postulates to confirm their etiology. To ensure accurate identification of the pathogens, we integrated the traditional morphological characterization approach and the modern molecular multigene phylogenetic tree method. Subsequently, the sensitivity of several fungicides was determined in the laboratory, and the optimum inhibitor was identified. These findings can aid in the prevention and control of pitaya stem rot not only in the Guizhou Province but also in the neighboring regions.

2. Materials and Methods

2.1. Collection, Isolation, and Conservation

Stem rot branch samples were collected from a dragon fruit cultivation area in Zhenfeng and Luodian, Guizhou Province. The junction of diseased and healthy tissue was cut into 5 mm × 5 mm pieces, followed by disinfection with 0.1% mercury for 30 s. Subsequently, they were immersed in 75% ethanol for 5 s, rinsed thrice with sterile water, and dried on a sterile absorbent paper. The isolates were obtained by incubating the cleaned disease samples at 26 °C for 2–3 d at the center of a 9-cm-diameter potato glucose agar (PDA) medium. Next, they were purified using marginal mycelia or single hyphal culture methods. All isolates were stored in freezer tubes containing 20% (v/v) glycerol at –20 °C in the dark.

2.2. Koch ' s Postulates

The pure fungal strains were inoculated on PDA or oatmeal agar (OA) medium and cultivated at 26 °C for 7 d to generate a substantial quantity of conidia. The conidia were adequately collected by rinsing the colony multiple times with sterile water. The conidial concentration was measured using a hemocytometer and subsequently adjusted to 1×10^6 conidia/mL with sterile water. Healthy dragon fruit stem blocks were transplanted into 1.8-L pots filled with deionized water-saturated sterilized substrate soil. The spore suspension (200 μL) was then shallowly injected into the healthy dragon fruit branches and moistened with absorbable cotton after approximately a week of stem growth. Each group comprised five branches. The control treatments were inoculated with equal amounts of sterile water. Finally, all treatment samples were planted in an artificial climate chamber with a 12/12 h light/dark cycle, a relative humidity of approximately 80%, and a temperature of 26 °C. After 21 d, disease incidence was observed and recorded, and the diseased roots were placed on the PDA medium for pathogens to be re-isolated and identified.

 doi:10.20944/preprints202310.1930.v1

2.3. Morphological Studies

Microscopic characteristics, such as colony shape and color, were visually observed on a 7-d-old PDA culture. Moreover, microscopic characteristics, such as conidia shape and size, were observed using a microscope after culturing on a slide. A 1-cm square OA medium containing mycelia was cut and placed on a sterile slide, followed by a clean 1-cm square OA medium on each side, with a cover glass placed on top of them. This simple apparatus was then placed in a Petri dish covered with sterile filter paper and moistened with a small amount of sterile water. Finally, the petri dishes were sealed and cultured at 26 °C for approximately 7 d. The conidial characteristics of the slides and cover slides were observed under a microscope. The conidia and was photographed using a scanning electron microscope.

2.4. DNA Extraction, PCR Analysis, and Multi-Locus Phylogeny

Genomic DNA was extracted from the mycelia of all isolates using Rapid Fungal Genomic DNA Isolation Kit (B518229; Sangon Biotech, Shanghai, China) according to the manufacturer's instructions. Sequences of the ribosomal DNA internal transcribed spacer (ITS) region, translation elongation factor 1-alpha encoding gene (EF-1α), and the second largest subunit of the RNA polymerase II encoding gene (retinol-binding protein 2 [RPB2]) were used for species-level identification using the primer sets listed in Table 1. A Rapid Fungi Genomic DNA Isolation kit (B518229, Sangon Biotech, Shanghai, China) was used to prepare the PCR mixes, which had a total volume of 25 L (Table 1) [22–24]. Next, amplification was conducted using a PCR instrument (846-x-070-723, Analytik Jena, Gottingen, Germany). A 2% agarose gel containing a nucleic acid dye was used to segregate the amplification products, which were subsequently photographed under UV light. The validated PCR products were sent to Sangon Biotech (Shanghai, China) for Sanger sequencing. The original sequence was downloaded, analyzed, integrated, and submitted to GenBank. Phylogenetic trees were constructed via the CIPRES web portal using the Maximum Likelihood (ML) method employing the combined ITS, EF-1α and RPB2 dataset (https://www.phylo.org/portal2/login!input.action) (Table S1). The species of F. sacchari was selected as outgroups. The RAxML-HPC BlackBox program was used with its default parameters for the ML analysis.

Table 1. The PCR primers and PCR systems used in this study.

			PCR mixtures （25 μL）					**PCR conditions**				
								35 cycles				
PCR regions	**Primers (5'-3')**		2× Phanta Max Buffer	DNA Polymerase	dNTP Mix	Each primer	Predenaturation	denaturation	annealing	extension	Final extension	**References**
ITS	ITS4	GGAAGTAAAAGTCGTAACAAGG							55°C for 15 s			[22]
	ITS5	TCCTCCGCTTATTGATATGC										
EF1-a	EF1	ATGGGTAAGGARGACAAGAC	1×	1 U	0.2 mM	0.2 μM	94°C for 3 min	94°C for 15 s	60°C for 15 s	72°C for 1 min	72°C for 5 min	[23]
	EF2	GGARGTACCAGTSATCATGTT										
RPB2	rpb2-5f	GAYGAYMGWGATCAYTTYGG							51°C for 15 s			[24]
	rpb2-7cr	CCCATRGCTTGYTTRCCCAT										

2.5. Metabolic Profiling in the Biolog FF MicroPlate

For species identification, metabolic analysis of fungi was performed on Biolog FF microplates (1006) containing 95 different carbon sources [25]. The isolates were inoculated on PDA medium at

 doi:10.20944/preprints202310.1930.v1

26 °C for 7 d to generate a considerable quantity of mycelia. The mycelia were gently dipped in a sterile cotton swab and transferred to a test tube containing FF-IF solution. The absorbance of fungal suspension was adjusted to 75% ± 2% at 490 nm using a turbidimeter. A 100 μL suspension was then added to each well of the Biolog FF microplate and incubated at 26 °C. The microplates were removed every 12 h, placed in a MicroStation readout, and measured at 490 nm (mitochondrial activity) and 750 mm (mycelium growth) using the MicrologTM 3 software.

2.6. Fungicide Sensitivity Testing

Eight common fungicides were selected for the in vitro toxicity analysis of strains H-4 and H-5 (Table 2). Five distinct concentrations of antibiotic PDA medium were established by dissolving and diluting each fungicide with sterile water and then absorbing and adding various volumes of the liquid to the PDA medium (Table 2). All prepared solutions were poured into 9-cm diameter sterile Petri dishes. The center of each dish was inoculated with a 5-mm diameter mycelium disk cut using a hole punch. A PDA medium without fungicides was used as the control. Each treatment was replicated thrice. All dishes were cultured for 8 d at 26 °C, and the colony diameter was measured and recorded using the cross method.

Table 2. Concentration gradient of different eight fungicides used for inhibitory test.

Fungicides	Concentration (μg/mL)					Manufacturer
	C1	C2	C3	C4	C5	
250 g/L Azoxystrobin	1	2	4	6	8	Syngenta Nantong Crop Protection Co., Ltd., Jiangsu, China
325 g/L Difenoconazole·azoxystrobin	0.5	1	2	5	10	Syngenta Nantong Crop Protection Co., Ltd., Jiangsu, China
300 g/L Difenoconazole·propiconazole	0.2	0.5	1	2	4	Syngenta Nantong Crop Protection Co., Ltd., Jiangsu, China
25 g/L Fludioxonil	1	2	4	6	8	Syngenta Nantong Crop Protection Co., Ltd., Jiangsu, China
40% Difenoconazole	0.2	0.5	1	2	4	Shandong Dongtai Agrochemical Co., Ltd., Shandong, China
75% Trifloxystrobin·tebuconazole	0.2	0.5	1	2	4	Bayer Aktiengesellschaft, Chengdu,China
50% Varbendazim	0.01	0.05	0.1	0.5	1	Sichuan Guoguang Agrochemical Co., Ltd., Chengdu,China
45% Lime Sulphur	0.05	0.1	0.5	1	2	Hebei Shuangji Chemical Co., Ltd., Hebei, China

The inhibitory effect of each fungicide on the growth of each isolate was calculated as follows:

$$\text{Inhibitory rate (\%)} = [(\Phi c - \Phi t) / (\Phi c - 5)] \times 100\% \quad (1)$$

where Φc is the diameter of the treated pathogen colony, Φt is the diameter of the pathogen colony in the control group, and 5 is the diameter of the inoculated mycelial disk.

2.7. Statistical Analysis

Microsoft Excel 2019 and GraphPad Prism 7 software were used for statistical analysis of the experimental data, and the concentration for 50% of maximum effect (EC_{50}) and regression equation correlation coefficient, r, were determined.

3. Results

3.1. Pathogenicity Test of the Isolated Strains

Twenty-four fungal isolates were obtained from dragon fruit stem rot. Based on their morphological characteristics and pathogenic potential, two isolates, H-4 and H-5, were further screened for pathogenicity using Koch's postulates. After 21 d of artificial inoculation with H-4 and H-5 conidia, noticeable brown rot occurred, which was consistent with the field symptoms (Figure

Preprints (www.preprints.org) | NOT PEER-REVIEWED | Posted: 1 November 2023 doi:10.20944/preprints202310.1930.v1

1). However, plants in the control group exhibited no disease symptoms (Figure 1). The pathogens were isolated and confirmed to be consistent in the diseased tissue of all inoculated plants. Therefore, isolates H-4 and H-5 were confirmed as the pathogens responsible for stem rot in dragon fruit.

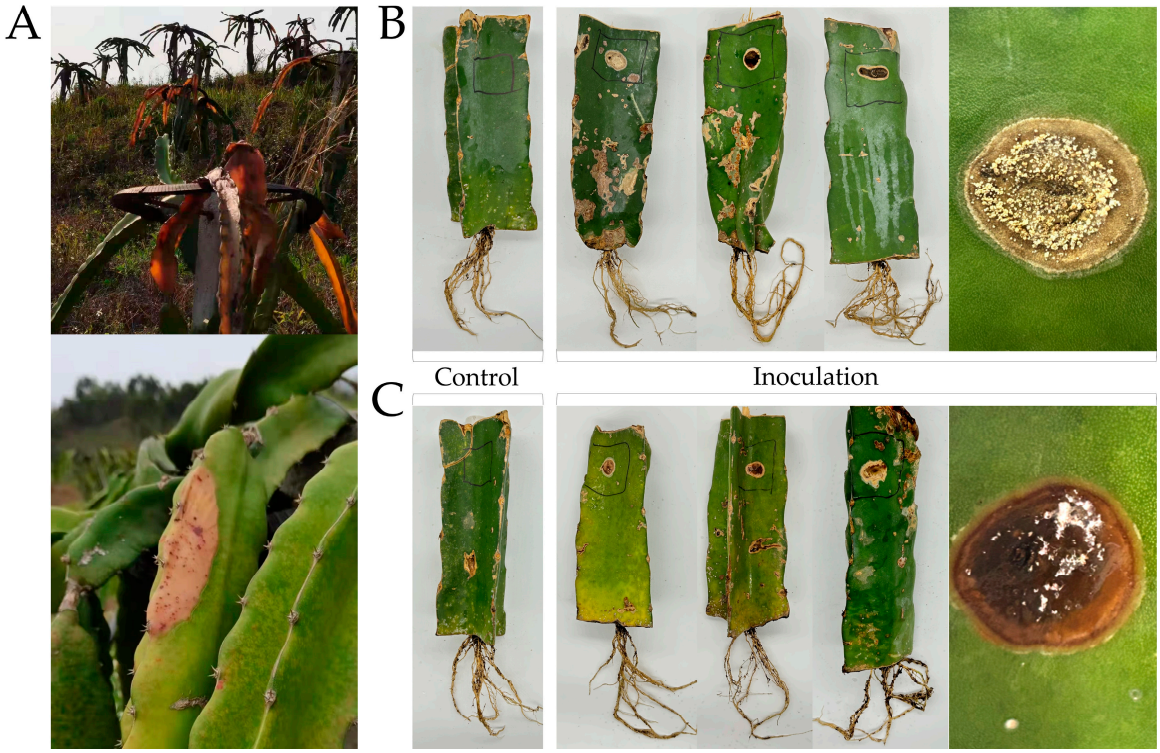

Figure 1. The symptoms of stem rot on dragon fruit. (A) Symptoms in field; (B) Pathogenicity test results on stem inoculated with sterile water or the isolate H-4; (C) Pathogenicity test results on stem inoculated with sterile water or the isolate H-5.

3.2. Isolate Identification

The pathogenic strains, H-4 and H-5, were cultured on a PDA medium and slides of OA medium for morphological identification. These two isolates exhibited rapid growth on PDA, with branched mycelium containing septa. The aerial mycelium appeared white, with a creamy to yellowish pigment (Figures 2A and 3A). Conidial characteristics were observed on the slides. For the H-4 strain, the microconidia were oval with either no septa or one septum, measuring 20.14-(11.65)-8.53 × 6.16-(4.65)-2.54 μm (Figure 2B–C). Macroconidium typically possessed three septa, which were slender, sickle-shaped to nearly straight, with a diameter of 35.34-(23.32)-18.16 × 4.89-(3.87)-3.10 μm (Figure 2D–F). For the H-5 strain, the microconidia were oval with either no septa or one septum, measuring 14.34-(9.65)-7.53 × 6.06-(4.15)-2.04 μm (Figure 3B–C). Macroconidia were observed with 3 to 5 septa, with a diameter of 65.43-(43.53)-36.76 × 4.83-(3.67)-3.03 μm (Figure 3D–E).

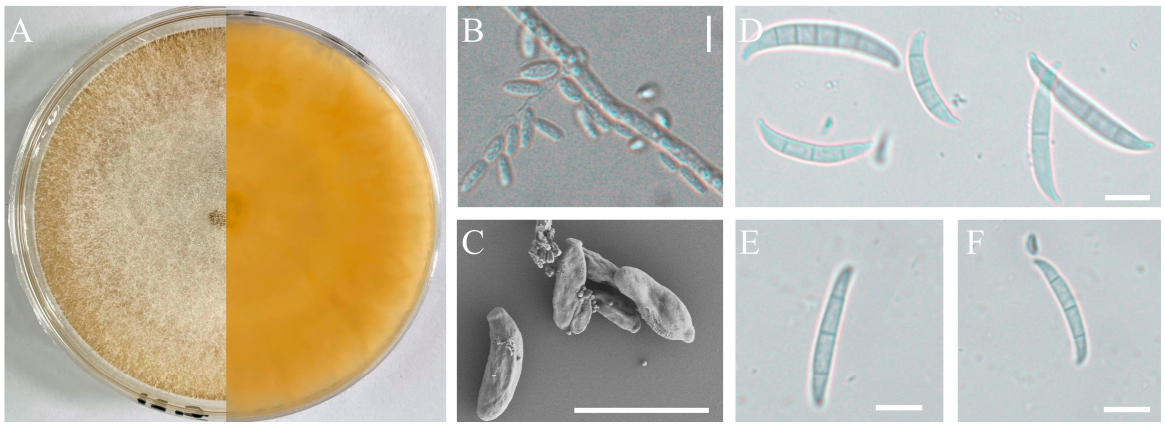

Preprints (www.preprints.org) | NOT PEER-REVIEWED | Posted: 1 November 2023 doi:10.20944/preprints202310.1930.v1

Figure 2. Morphological characteristics of the isolate H-4. Front and back of the colony (A); Microconidia observed by optical microscopy (B) or Scanning electron microscope (C); Macroconidia observed by scanning electronic microscopy (SEM, SU8100, Japan) (D–F); scale bars: 10 μm.

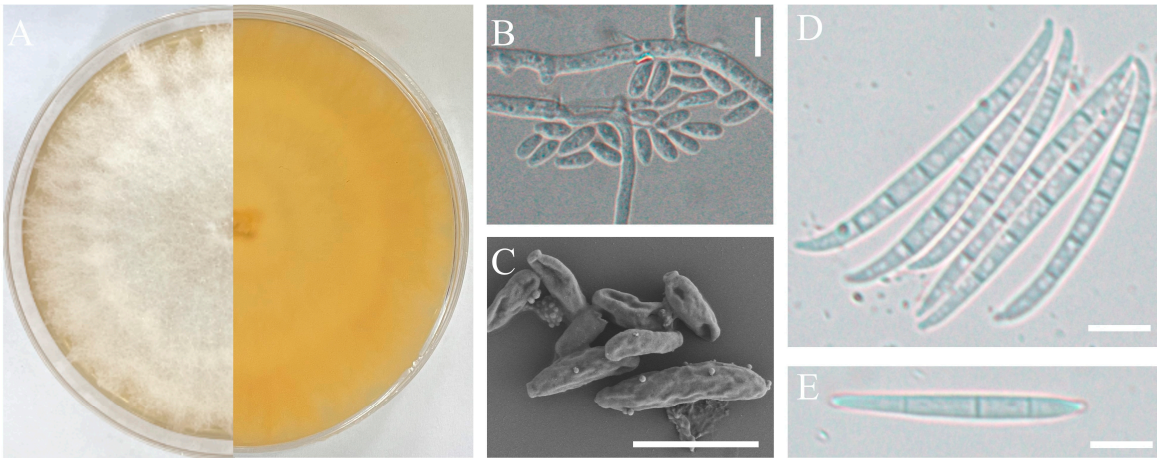

Figure 3. Morphological characteristics of the isolate H-5. Front and back of the colony (A); Microconidia observed by optical microscopy (B) or Scanning electron microscope (C); Macroconidia observed by optical microscopy (D,E); scale bars: 10 μm.

For molecular identification, three distinct fragments of ITS, EF-1α and RPB2 from strains H-4 and H-5 were sequenced and subsequently submitted to the NCBI database (Table S1). The corresponding sequences of related species were collected, including that of F. *sacchari as* an outgroup. A phylogenetic tree was constructed using the ML method. The results indicated that the H-4 isolate exhibited the least connection to the phylogenetic cluster containing F. *oxysporum*, with a confidence rate exceeding 97% (Figure 4). The H-5 isolate was located on the same branch as F. *concentricum* (Figure 5) and demonstrated a 100% support rate.

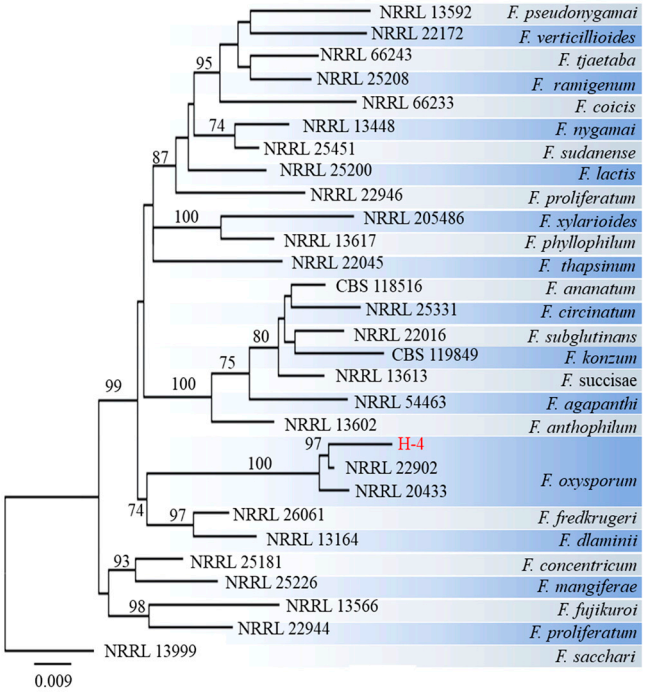

Figure 4. Maximum Likelihood (ML) tree of the isolate H-4 was generated based on internal transcribed spacer (ITS), translation elongation factor 1-alpha encoding gene (*EF-1α*), and the second

Preprints (www.preprints.org) | NOT PEER-REVIEWED | Posted: 1 November 2023 doi:10.20944/preprints202310.1930.v1

largest subunit of RNA polymerase II encoding gene (*RPB2*) gene sequences. Numbers on the branches represent bootstrap values (BVs) greater than 70%.

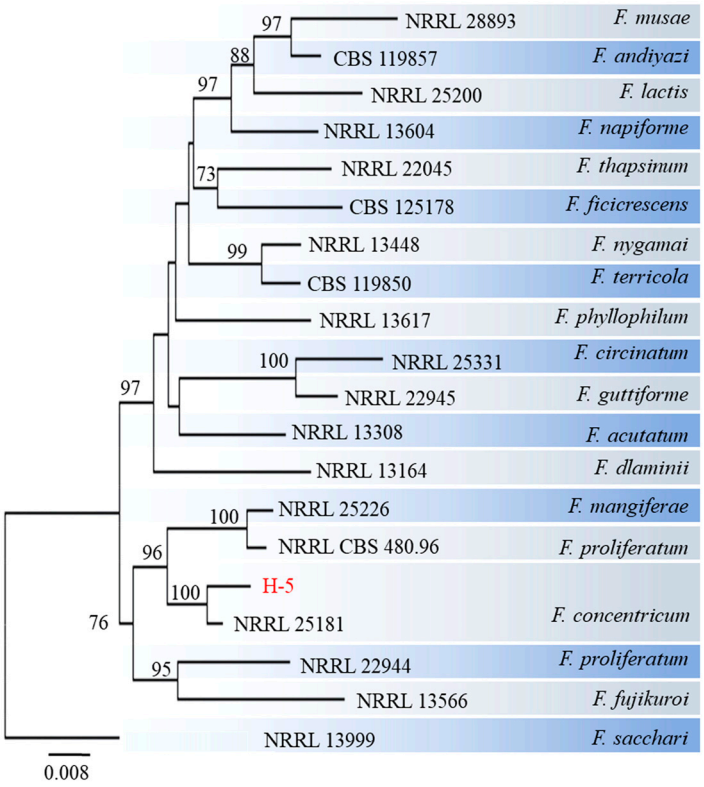

Figure 5. Maximum Likelihood (ML) tree of the isolate H-5 was generated based on internal transcribed spacer (ITS), translation elongation factor 1-alpha encoding gene (*EF-1α*), and the second largest subunit of RNA polymerase II encoding gene *(RPB2*) gene sequences. Numbers on the branches represent bootstrap values (BVs) greater than 70%.

The metabolic abilities of both isolates were assessed using a Biolog FF MicroPlate, which encompasses 95 different carbon sources. The H-4 isolate demonstrated proficiency in utilizing 74 carbon sources for full growth. However, it demonstrated incapacity in utilizing 21 carbon sources, including dextrin, gentiobiose, A-cyclodextrin, and ß-cyclodextrin, resulting in no growth. The H-5 isolate was responsive to 85 carbon sources but showed insensitivity to ten, including gluconamide, adenosine-5'monophosphate, ltose, and maltitol (Table 3).

Table 3. Carbon source metabolism of the isoaltes on FF microplatasa.

Substrates	Isolates		Substrates	Isolates		Substrates	Isolates	
	H-4	H-5		H-4	H-5		H-4	H-5
Water	−*	−	a-Cyclodextrin	−	−	a-D-Glucose-1 - Phosphate	+	+
Tween 80	+−	+	ß-Cyclodextrin	−	−	N-Acetyl-ß-D-Glucosamine	−	+−
Glycerol	+−	+	Glucuronamide	+	−	D-Glucuronic Acid	+	+−
Dextrin	−	+−	i-Erythritol	+	+−	N-Acetyl-D-Galactosamine	+−	+−
Glycogen	+	+	D-Fructose	−	+−	N-Acetyl-ß-D-Mannosamine	−	−
Adonitol	+−	+−	L-Fucose	+	+−	m-Inositol	+−	+
Amygdalin	+−	+−	D-Galactose	−	+−	2-Keto-D-Gluconic Acid	+	+
D-Arabinose	−	+−	D-Galacturonic Acid	−	+−	a-D-Lactose	+	+−
L-Arabinose	−	+−	Gentiobiose	−	+−	Lactulose	−	−
D-Arabitol	−	+−	D-Gluconic Acid	+	+−	Maltitol	+−	−

 doi:10.20944/preprints202310.1930.v1

Arbutin	+−	+	D-Glucosamine	−	+−	Maltose	−	+−
D-Cellobiose	−	+	a-D-Glucose	−	+−	Maltotriose	+−	+−
D-Mannitol	+	+	D-Ribose	+	+−	y-Aminobutyric Acid	+	+
D-Mannose	−	+−	Salicin	+	+−	Bromosuccinic Acid	+	+
D-Melezitose	+−	+−	Sedoheptulosan	+	+−	a-Methyl-D-Galactoside	+	−
D-Melibiose	+	+−	D-Sorbitol	+	+−	ß-Hydroxybutyric Acid	+	+
Fumaric Acid	+	+	L-Sorbose	+	+−	y- Hydroxybutyric Acid	+	+
L-Lactic Acid	+	+	Stachyose	+	+−	p-Hydroxy-phenylacetic Acid	+	+
D-Malic Acid	+	+	Sucrose	+	+−	a-Ketoglutaric Acid	+	+
L-Malic Acid	+	+	D-Tagatose	−	+−	D-Lactic Acid Methyl Ester	+	+
Quinic Acid	+	+	D-Trehalose	+	+−	ß-Methyl-D-Galactoside	+	+
D-Psicose	+−	+	Turanose	+	+−	a-Methyl-D-Glucoside	+	+−
D-Raffinose	+	+	Xylitol	+	+−	ß-Methyl-D-Glucoside	+−	+−
L-Rhamnose	+	+	D-Xylose	+	+−	Palatinose	−	+−
L-Proline	+	+	L-Alanine	+−	+−	L-Phenylalanine	+	+
Sebacic Acid	−	+	L-Alanyl-Glycine	+	+−	D-Saccharic Acid	+	+
Succinamic Acid	+	+	L-Asparagine	+	+−	L-Pyroglutamic Acid	+	+
Succinic Acid	+	+	L-Aspartic Acid	+	+−	Succinic Acid Mono-Methyl Ester	−	+
L-Serine	+	+	L-Glutamic Acid	+	+−	N-Acetyl-L-Glutamic Acid	+−	+−
L-Threonine	+	+	Gycyl-L-Glutamic Acid	+	+−	2-Aminoethanol	+	+
Uridine	+	+	L-Ornithine	+	+−	Putrescine	+	+
Adenosine	+	+	L-Alaninamide	+	+−	Adenosine-5′-Monophosphate	+	−

* "+" sensitive; "−" insensitive; "+−" weakly sensitive.

Therefore, based on the analysis of morphology, molecular systematics, and metabolic characteristics, H-4 and H-5 were identified as F. *oxysporum* and F. *concentricum*, respectively. Notably, this study is the first to identify F. *concentricum* as a causative pathogen of stem rot in dragon fruit.

3.3. Fungicidal Efficacy on the Isolates

The growth of the two pathogenic isolates was assessed using a medium containing eight fungicides; the results revealed varying degrees of inhibitory effects (Table 4). For H-4, trifloxystrobin·tebuconazole exhibited the strongest inhibitory impact, with an EC_{50} of 0.1262 μg/mL, followed by difenoconazole·azoxystrobin (0.1775 μg/mL) and difenoconazole (0.1794 μg/mL). Azoxystrobin and lime sulfur exhibited the worst inhibitory effect, with EC_{50} values of 10.6462 μg/mL and 5.2869 μg/mL, respectively (Table 4). For H-5, the fungicide effect was similar to that of H-4, with trifloxystrobin·tebuconazole as the most effective, with an EC_{50} of 0.1385 μg/mL, and lime sulfur and azoxystrobin (3.5874 μg/mL and 2.8217 μg/mL, respectively) as the least effective (Table 4).

Table 4. In vitro toxicity of eight fungicides against the isolates.

Isolates	Fungicides	Regression equation	Correlation coefficient (r)	EC_{50} (μg/mL)
H-4	250 g/L Azoxystrobin	y = 0.039x + 4.5848	0.8851	10.6462
	325 g/L Difenoconazole·azoxystrobin	y = 0.0728x + 5.3881	0.8389	0.1775
	300 g/L Difenoconazole·propiconazole	y = 0.2128x + 5.556	0.7749	0.3789
	25 g/L Fludioxonil	y = 0.0279x + 5.3592	0.9683	1.146
	40% Difenoconazole	y = 0.2409x + 6.2693	0.9127	0.1794
	75% Trifloxystrobin·tebuconazole	y = 0.1525x + 5.5243	0.9272	0.1262
	50% Varbendazim	y = 8.6653x - 2.7422	0.8983	0.8935
	45% Lime Sulphur	y = 0.3168x + 3.3251	0.9495	5.2869
H-5	250 g/L Azoxystrobin	y = 0.0757x + 4.7864	0.9795	2.8217
	325 g/L Difenoconazole·azoxystrobin	y = 0.1081x + 5.2067	0.8992	0.4225
	300 g/L Difenoconazole·propiconazole	y = 0.1948x + 5.3253	0.7525	1.062
	25 g/L Fludioxonil	y = 0.0584x + 5.3219	0.8337	0.9573
	40% Difenoconazole	y = 0.1252x + 5.8584	0.9741	0.4606
	75% Trifloxystrobin·tebuconazole	y = 0.3768x + 4.9478	0.8562	0.1385

 doi:10.20944/preprints202310.1930.v1

50% Varbendazim	y = 1.257x + 3.6195	0.8196	1.098
45% Lime Sulphur	y = 0.6335x + 2.7274	0.4635	3.5874

4. Discussion

Over the past two decades, the expansion of dragon fruit cultivation in Guizhou Province has led to a significant escalation in the severity of stem rot. *Fusarium proliferatum* was identified as the fungal pathogen of postharvest diseases on dragon fruits [6]. In this study, we collected a large number of disease samples from multiple planting sites and through pathogen isolation, 24 strains were obtained. In addition to F. *proliferatum* isolates, numerous other isolates were also obtained. Subsequently, two isolates, H-4 and H-5, exhibiting differences and potential pathogenicity, were selected for further disease-related research. This selection was based on preliminary morphological observations and assessment of ITS sequencing.

Currently, the most effective method for confirming pathogenicity, following Koch's postulates, involves the inoculation of live plants with a spore suspension [26]. Stem rot usually occurs under hot and humid weather conditions, as this elevated humidity provides an environment conducive to the formation, germination, and infection of plant tissues by fungal spores. Therefore, high humidity is considered an important factor in the occurrence of this disease [27]. Thus, we implemented a treatment involving sterile cotton impregnated with moisture to establish a suitable environment for disease occurrence.

Microorganism identification is a fundamental and crucial aspect of microbiology research. Currently, molecular biology techniques have reached an unprecedented level of development and maturity, rendering the combination of molecular biology and traditional morphology the standard process of identification [28–30]. In this study, a large number of macroconidial structures suspected to belong to the *Fusarium* genus were identified through microscopic observation of tissue slides from lesions. Moreover, relevant characteristics of the *Fusarium* genus were also identified in the purified culture. Therefore, two isolates were identified based on relevant morphological characteristics of Fusarium, including macroconidium, microconidium, colony, and mycelium morphology. For molecular biology identification, three gene fragments, namely ITS, EF-1α and RPB2, were selected for the construction of a polygenic molecular developmental tree for homology analysis. The results revealed that the two isolates were clearly clustered in F. *oxysporum* and F. *concentricum*. Furthermore, a comprehensive study of the pathogens was conducted using 95 different biochemical tests on FF microplates. This investigation revealed that although the types of carbon sources used by the two isolates differed, they demonstrated proficiency in utilizing a majority of the carbon sources, indicating that both isolates exhibited strong environmental survival abilities.

Stem rot occurs worldwide and stands as a major limitation to the development of the dragon fruit industry. In Guizhou Province, we identified both the previously known pathogen, F. *oxysporum*, and a newly discovered pathogen, F. *concentricum* [31]. Both pathogens exhibited the ability to produce macroconidia and microconidia that can be disseminated through the wind or rain, resulting in widespread disease outbreaks [32]. To effectively prevent and control this disease, we conducted laboratory experiments to evaluate the inhibitory effects of eight chemical agents on the growth of these pathogens. The results revealed that 75% trifloxystrobin·tebuconazole exhibited the strongest inhibitory effect on both H-4 and H-5 isolates. Notably, the concentration gradient of the experimental agents used in this study was only appropriate for laboratory screening; therefore, additional studies are required to determine the actual control efficacy and application concentration in field production. Furthermore, the experimental design for virulence determination focused on only a select few common chemical agents available in the market. Thus, additional research is warranted to explore their combined virulence determination, mixing proportions, and control effects [33]. Moreover, a comprehensive analysis of the impacts of the use of chemicals in field production on economic, social, and environmental benefits is imperative.

5. Conclusions

In this study, we investigated the causative pathogenic fungi responsible for dragon fruit stem rot in Guizhou Province. Following Koch's postulates, we identified two isolates as the causative pathogens for this disease. Through morphological observations and molecular identification, we determined these two strains to be F. oxysporum and F. concentricum. Simultaneously, an experimental investigation using FF microplates showed that both isolates could utilize a wide range of carbon sources. To provide an important contribution to the field management and prevention of this disease, we examined the inhibitory effects of eight fungicides on both pathogens. Our findings revealed that 75% trifloxystrobin·tebuconazole exhibited the strongest inhibitory effect on the mycelium growth of the pathogens. These findings bear substantial promise in directing the efficient management of stem rot in dragon fruit in Guizhou, China.

Supplementary Materials: The following supporting information can be downloaded at the website of this paper posted on Preprints.org. Table S1: A list of species, isolates, and GenBank accession numbers of sequences used in this study.

Author Contributions: Jin Zhao: Conceptualization, Methodology, Formal analysis, Writing–original draft, Writing–editing; Miao Huang: Conceptualization, Methodology, Formal analysis.

Funding: This research was funded by the Regional Fund of the National Natural Science Foundation of China (32260799); Outstanding Young Scientist Program of Guizhou Province under grant number KY [2021]028, Cultivation Research Program of Guizhou University under grant numbers [2019]42.

Data Availability Statement: All relevant data are within the paper. And more information can be found in the references.

Conflicts of Interest: The authors declare no conflict of interest.

References

1. Ibrahim, S.R.M.; Mohamed, G.A.; Khedr, A.I.M.; Zayed, M.F.; El-Kholy, A.A.E.S. Genus Hylocereus: Beneficial phytochemicals, nutritional importance, and biological relevance—A review. *Journal of Food Biochemistry* **2018**, *42*(2), e12491. DOI：10.1111/jfbc.12491
2. Arivalagan, M.; Karunakaran, G.; Roy, T.K.; Dinsha, M.; Sindhu, B.C.; Shilpashree, V.M.; Satisha, G.C.; Shivashankara, K.S. Biochemical and nutritional characterization of dragon fruit (*Hylocereus* species). *Food Chemistry* **2021**, *353*, 129426. DOI: 10.1016/J.FOODCHEM.2021.129426
3. Liaotrakoon, W.; De Clercq, N.; Van Hoed, V.; Van de Walle, D.; Lewille, B.; Dewettinck, K. Impact of thermal treatment on physicochemical, antioxidative and rheological properties of white-flesh and red-flesh dragon fruit (*Hylocereus* spp.) purees. *Food and Bioprocess Technology* **2013**, *6*, 416-430. DOI：10.1007/s11947-011-0722-4
4. Pan, L.; Fu, J.; Zhang, R.; Qin, Y.; Lu, F.; Jia, L.; Hu, Q.; Liu,C. ; Huang, L.; Liang, G. Genetic diversity among germplasms of pitaya based on SSR markers. *Scientia Horticulturae* **2017**, *225*, 171-176. DOI：10.1016/j.scienta.2017.06.053
5. Zhao, Y.; Yang, S.; Jiang, L.; Yang, Q.; Luo, L.; Jiang, J.; Malichan, S.; Zhao, J.; Xie, X. Pitaya virus X coat protein acts as an RNA silencing suppressor and can be used as specific target for detection using RT-LAMP. *Plant Disease* **2023**, (ja). DOI：10.1094/PDIS-11-22-2570-SC
6. Li, Y.; Chen, H.; Ma, L.; An, Y.; Wang, H.; Wu, W. Laboratory screening of control agents against isolated fungal pathogens causing postharvest diseases of pitaya in Guizhou, China. *Frontiers in Chemistry* **2022**, *10*, 942185.
7. Xu, M.;Liu, C.L.;,Luo, J.; Qi, Z.; Yan, Z.; Fu, Y.; Wei, S.S.; Tang, H. Transcriptomic de novo analysis of pitaya (*Hylocereus polyrhizus*) canker disease caused by *Neoscytalidium dimidiatum*. *BMC genomics* **2019**, *20*(1), 1-16. DOI：10.1186/s12864-018-5343-0
8. Balendres, M.A.; Bengoa, J.C. Diseases of dragon fruit (*Hylocereus* species): Etiology and current management options. *Crop protection* **2019**, *126*, 104920. DOI：10.1016/j.cropro.2019.104920
9. Hong, C.F.; Gazis, R.; Crane, J.H.; Zhang, S. Prevalence and epidemics of *Neoscytalidium* stem and fruit canker on pitahaya (*Hylocereus* spp.) in South Florida. *Plant disease* **2020**, *104*(5), 1433-1438. DOI：10.1094/PDIS-10-19-2158-RE

10. Mohd, M.H.; Salleh, B.; Zakaria, L. An overview of fungal diseases of pitaya in Malaysia. In *Proceeding of Improving Pitaya Production and Marketing Workshop* **2015**, September). (pp. 13-15).
11. Zhang, R.Y.; Zhao, S.X.;, Tan, Z.Q.; Zhu, C.H. First report of bacterial stem rot disease caused by *Paenibacillus polymyxa* on *Hylocereus undulatus* in China. *Plant Disease* **2017**, *101*(6), 1031-1031. DOI：10.1094/pdis-11-16-1577-pdn
12. Wakchaure, G.C.; Kumar, S.; Meena, K.K.; Rane, J.; Pathak, H. Dragon fruit cultivation in India: scope, constraints and policy issues. *Technical Bulletin* **2021**, *27*, 47.
13. Rita, W.S.; Suprapta, D.N.; Sudana, I.M.; Swantara, I.M.D. First report on *Fusarium solani*, a pathogenic fungus causing stem rot disease on dragon fruits (*Hylocereus* sp.) in Bali. *Journal of Biology, Agriculture and Healthcare* **2013**, *3*(17), 93-99. ISSN: 2224-3208
14. Retana-Sánchez, K.; Castro-Zúñiga, O.; Blanco-Meneses, M.; Quesada-González, A. Etiology of stem rot on *Hylocereus* spp. cause by *Enterobacter hormaechei* in Costa Rica. *Agronomía Costarricense* **2019**, *43*(2), 61-73. http://dx.doi.org/10.15517/rac.v43i2.37949.
15. Paugh, K.R.; Gordon, T.R. The Population of *Fusarium oxysporum* f. sp. lactucae in California and Arizona. *Plant disease* **2020**, *104*(6), 1811 – 1816. https://doi.org/10.1094/PDIS-06-19-1228-RE
16. Xu, M.; Peng, Y.; Qi, Z.; Yan, Z.; Yang, L.;,He, M.D.; Li, Q.X.; Liu, C.L.; Ruan, Y.Z.; Wei, S.S.; Xie, J.; Xia, Y.Q.; Tang, H. Identification of *Neoscytalidium dimidiatum* causing canker disease of pitaya in Hainan, China. *Australasian Plant Pathology* **2018**, *47*, 547-553. DOI: 10.1007/s13313-018-0588-2
17. Taguiam, J.D.; Evallo, E.; Bengoa, J.; Maghirang, R.; Balendres, M.A. Susceptibility of the three dragon fruit species to stem canker and growth inhibition of *Neoscytalidium dimidiatum* by chemicals. *Journal of Plant Pathology* **2020**, *102*, 1077-1084. DOI: 10.1007/s42161-020-00551-0
18. Noegrohati, S.; Sulasmi, S.; Hernadi, E.; Asviastuti, S. Dissipation pattern of azoxystrobin and difenoconazole in red dragon fruit (*Hylocereus polyrhizus*) cultivated in Indonesian highland (West Java) and coastal area (DI Jogyakarta) and its implication for dietary risk assessment. *Food Quality and Safety* **2019**, *3*(2), 99-106. DOI: 10.1093/fqsafe/fyz009
19. Wedge, D.E.; Elmer, W.H. Fusarium wilt of orchids. *Icogo Bull* **2008**, *2*(3), 9-10.
20. Hudson, O.; Waliullah, S.; Ji, P.; Ali, M.E. Molecular characterization of laboratory mutants of *Fusarium oxysporum* f. sp. niveum resistant to prothioconazole, a demethylation inhibitor (DMI) fungicide. *Journal of Fungi* **2021**, *7*(9), 704. DOI: 10.3390/JOF7090704
21. Wang, Y.F.; Hao, F.M.; Zhou, H.H.; Chen, J.B.; Su, H.C.; Yang, F.; Cai, Y.Y.; Li, G.L.; Zhang, M,; Zhou, F. Exploring potential mechanisms of fludioxonil resistance in *Fusarium oxysporum* f. sp. melonis. *Journal of Fungi* **2022**, *8*(8), 839. DOI: 10.3390/JOF8080839
22. White, T.J.; Bruns, T.; Lee, S.J.W.T.; Taylor, J. Amplification and direct sequencing of fungal ribosomal RNA genes for phylogenetics. In PCR Protocols: A Guide to Methods and Applications; Academic Press: Cambridge, MA, USA, 1990; Volume 18, pp. 315–322.
23. Bischoff, J.F.; Rehner, S.A.; Humber, R.A. A multilocus phylogeny of the Metarhizium anisopliae lineage. *Mycologia* **2009**, *101*:512–530. DOI: 10.3852/07-202
24. Liu, Y.J.; Whelen, S.; Hall, B.D. Phylogenetic relationships among ascomycetes: Evidence from an RNA polymerse II subunit. *Molecular Biology & Evolution* **1999**, 16, 1799–1808. DOI: 10.1016/S0723-2020(11)80145-1
25. Buyer, J.S.; Roberts, D.P.; Millner, P.; Russek-Cohen, E. Analysis of fungal communities by sole carbon source utilization profiles. *J Microbiol. Meth* 2001, **45**(1), 53–60. DOI: 10.1016/S0167-7012(01)00221-4
26. Chai, X.; Yang, Z.; Fu, Q.; Pan, B.Z.; Tang, M.; Li, C.; Xu, Z.F. First report of root and basal stem rot in sacha inchi (*Plukenetia volubilis*) caused by *Fusarium oxysporum* in China. *Plant Disease* **2018**, *102*(1), 242-242. DOI: 10.1094/PDIS-06-17-0784-PDN
27. Manstretta, V.; Rossi, V. Effects of temperature and moisture on development of *Fusarium graminearum* perithecia in maize stalk residues. *Appl. Environ. Microbiol* **2015**, *82*(1), 184–191. DOI: 10.1128/AEM.02436-15
28. Trevine, V.C.; Grazziotin, F.G.; Giraudo, A.; Sallaberry-Pincheira, N.; Vianna, J.A.; Zaher, H. The systematics of Tachymenini (Serpentes, Dipsadidae): An updated classification based on molecular and morphological evidence. *Zoologica Scripta* **2022**, *51*(6), 643-663. DOI: 10.1111/ZSC.12565
29. Hafizi, R.; Salleh, B.; Latiffah, Z. Morphological and molecular characterization of *Fusarium. solani* and F. *oxysporum* associated with crown disease of oil palm. *Brazilian Journal of Microbiology* **2013**, *44*, 959-968. DOI: 10.1590/S1517-83822013000300047

30. Du, Q.; Duan, C.X.; Li, S.C.; Tang, Z.L.; Luo, J.Y. First report of maize ear rot caused by *Fusarium concentricum* in China. *Plant Disease* **2020**,*104*(5), 1539. DOI: 10.1094/pdis-07-19-1515-pdn
31. Chen, Y.; Yan, W.; Xiao, M.; Xiao, T.; Zhao, Z.; Wang, H. Identification on pathogenic fungi of dragon fruit stem rot disease (in Chinese). *Molecular Plant Breeding* **2019**, *17*(3), 904-909. doi:10.13271/j.mpb.017.000904.
32. Caplin, I.; Unger, D.L. Molds on the Southern California deserts. *Annals of Allergy* **1983**, *50*(4), 260–263.
33. Khaledi, N.; Taheri, P.; Falahati, R.M. Identification, virulence factors characterization, pathogenicity and aggressiveness analysis of *Fusarium* spp., causing wheat head blight in Iran. *European Journal of Plant Pathology* 2017, *147*, 897-918. DOI: 10.1007/s10658-016-1059-7